

# 1 Characterization of hydrochars produced by hydrothermal 2 carbonization of rice husk

3  
4 **D. Kalderis<sup>1</sup>, M. S. Kotti<sup>1</sup>, A. Méndez<sup>2</sup>, and G. Gascó<sup>3</sup>**

5 [1] {Department of Environmental and Natural Resources Engineering, Technological and  
6 Educational Institute of Crete, Chania, 73100 Crete, Greece}

7 [2] {Departamento de Ingeniería de Materiales. E.T.S.I. Minas. Universidad Politécnica de  
8 Madrid, C/Ríos Rosas nº21, 28003 Madrid, Spain}

9 [3] {Departamento de Edafología. E.T.S.I. Agrónomos. Universidad Politécnica de Madrid,  
10 Ciudad Universitaria, 28004 Madrid, Spain}

11 Correspondence to: D. Kalderis (dkalderis@chania.teicrete.gr)

## 12 13 **Abstract**

14 Biochar is the carbon-rich product obtained when biomass, such as wood, manure or leaves, is  
15 heated in a closed container with little or no available air. In more technical terms, biochar is  
16 produced by so-called thermal decomposition of organic material under limited supply of  
17 oxygen (O<sub>2</sub>), and at relatively low temperatures (<700°C). Hydrochar differentiates from  
18 biochar because it is produced in an aqueous environment, at lower temperatures and longer  
19 retention times. This work describes the production of hydrochar from rice husks using a  
20 simple, safe and environmentally-friendly experimental set-up, previously used for  
21 degradation of various wastewaters. Hydrochars were obtained at 200°C and 300°C and at  
22 residence times ranging from 2 to 16 h. All samples were then characterized in terms of yield,  
23 surface area, pH, conductivity and elemental analysis and two of them were selected for  
24 further testing with respect to heating values and heavy metal content. The surface area was  
25 low for all hydrochars, indicating that porous structure was not developed during treatment.  
26 The hydrochar obtained at 300°C and 6 hrs residence times showed a predicted higher heating  
27 value of 17.8 MJ/kg, a fixed carbon content of 46.5% and a fixed carbon recovery of 113%,  
28 indicating a promising behaviour as a fuel.

1

2

### 3 **1 Introduction**

4 Subcritical water is hot water (100 - 374°C) under enough pressure to maintain the liquid  
5 state. It is an environmentally friendly and inexpensive solvent that exhibits a wide range of  
6 properties that renders it very effective in solvating and decomposing moderately polar or  
7 non-polar substances from a wide range of environmental matrices. Subcritical water can  
8 decompose naturally occurring substances and materials, such as complex amino acids,  
9 proteins and carbohydrates (sucrose, fructose and sorbose), sodium alginate, and brown coal,  
10 to produce more valuable and useful products. Additionally, subcritical water has been proved  
11 to decompose hazardous organic substances and materials such as pentachlorophenol (PCP),  
12 fluorochemicals, dioxins, polycyclic aromatic hydrocarbons (PAHs), polychlorinated  
13 biphenyls (PCBs) and polyvinyl chloride (PVC) (Kalderis et al., 2008 and references therein).

14 The hydrothermal treatment of biomass at temperatures in the range of 100–374°C gives rise  
15 to water soluble organic substances and a carbon-rich solid product, commonly known as  
16 hydrochar (Sevilla and Fuertes, 2009). Typically, the main components of biomass resources  
17 are 40-45 wt.% cellulose, 25-35 wt.% hemicellulose, 15-30 wt.% lignin and up to 10 wt.% for  
18 other compounds (Toor et al. 2011). The treatment of biomass in subcritical water has  
19 received considerable attention over the last few years. The degradation mechanisms of  
20 lignin, cellulose and hemi-cellulose during hydrothermal treatment and the effect of the  
21 experimental parameters (residence time, temperature, type of biomass) have been thoroughly  
22 described elsewhere (Sevilla and Fuertes, 2009, Jamari et al., 2012, Wahyudiono et al., 2012,  
23 Wiedner et al., 2013, Gao et al., 2013, Parshetti et al., 2013, Lu et al., 2013). The products  
24 obtained during treatment are gases (about 10% of the original biomass, mainly CO<sub>2</sub>), bio-oil  
25 consisting primarily of sugars, acetic acid, and other organic acids and the solid product (char)  
26 which contains about 41-90% of the mass of the original feedstock. The produced char has a  
27 higher energy density and is more hydrophobic than the original biomass. (Tufiq Reza et al.,  
28 2013).

29 Compared to other thermochemical processes such as pyrolysis, hydrogenation or  
30 gasification, aqueous conversion using subcritical water has the significant advantage of not  
31 requiring a drying process for feedstock and therefore can be conducted at high moisture  
32 content typical for biomass feedstocks. The hydrothermal carbonization temperature is

1 usually much lower than that of pyrolysis, gasification, and flash carbonization. The water  
2 present can be used as the reaction solvent, whereas at the same time some off-gases, such as  
3 CO<sub>2</sub>, nitrogen oxides, and sulfur oxides, are dissolved in water, forming the corresponding  
4 acids and/or salts, making further treatment for air pollution possibly unnecessary. Finally, it  
5 is an environmentally friendly method as it requires no additives and in most cases is simple  
6 to set-up and operate.

7 Compared to hydrochars, biochars produced through conventional pyrolysis methods have  
8 been more thoroughly applied and tested. Research on the applications of hydrochar is still in  
9 its early stages. Lately, hydrochars have been tested as soil conditioners and heavy metal  
10 immobilization means (Abel et al., 2013, Wagner and Kaupenjohann, 2014), as  
11 electrochemical supercapacitor electrode materials (Ding et al., 2013a, 2013b) and as anode  
12 materials for lithium ion batteries (Unur et al., 2013), with promising results. Undergoing  
13 work also focuses on their environmental impact and compatibility with agricultural and  
14 horticultural systems (Gajic and Koch, 2012, Busch et al., 2013, Bargmann et al., 2013).

15 Around 20% of the whole rice grain weight is rice husk. In 2008 the world rice grain  
16 production was 661 million tons and consequently 132 million tons of rice husk were also  
17 produced. While there are some established uses for rice husk, it is still considered a waste  
18 product in the rice mill industry and it is often either burned in the open or disposed of in  
19 landfills. Rice husk has been extensively studied for the production of activated carbon  
20 through conventional pyrolysis routes (Kalderis et al. 2008 and references therein), however,  
21 the studies that deal with hydrothermal carbonisation of rice husk are few. The scope of this  
22 study was to use a simple, safe, effective, environmentally-friendly method to produce  
23 hydrochars from rice husk and characterise the products. Two of the produced hydrochars  
24 were selected and their behaviour as fuels was examined.

25

## 26 **2 Materials and methods**

27 Rice husk (RH) was obtained from Janta Rice Mill in Gurdaspur (32.0333°N - 75.40°E) in  
28 India. Rice husk was initially washed thoroughly with water to remove any impurities, dried  
29 at 110°C for 6 h and then ground with a microhammer cutter mill and sieved 32 mesh (500  
30 µm) particle size. The properties of the feedstock material are shown in brief in Table 1 and  
31 described in detail in Kalderis et al., 2008.

1 The experiments described here are under static conditions i.e. no flow is required and no  
2 additional use of water. Additionally, monitoring of the process is not essential, since the  
3 oven can be pre-set at the required temperature and residence time. Finally, no pumping  
4 system is needed to maintain the system pressure, since pressure is automatically controlled  
5 by the steam/water equilibrium inside the reactor cell. The experimental set-up is described in  
6 detail in Kalderis et al. 2008 and Daskalaki et al. 2011. Briefly, one type of small laboratory  
7 reactor was used for hydrothermal treatment studies. The 25 ml reactors were constructed  
8 from (6-inches long, 0.64 inches i.d.) 316 stainless steel pipe with male national pipe threads  
9 (npt) and female end caps sealed with Teflon tape (Swagelok Company, USA).

10 A sample of the raw material was mixed with distilled water at a ratio of approximately 1/5.  
11 The mixture was then stirred and heated to become homogenized and impregnated at a  
12 temperature of 85°C until a thick uniform paste was obtained. A sample of wet rice husk paste  
13 (~75% moisture) was weighed before placing inside the reactor. Each reactor was loaded with  
14 25 g of wet paste. This procedure left ~5 ml of headspace in the cell. All static (non-flowing)  
15 reaction cells must contain a sufficient headspace so that the pressure inside the cell is  
16 controlled by the steam/liquid equilibrium. A full cell must never be used since the pressures  
17 could reach several thousand bar. The reactors were placed in a (pre-heated at the required  
18 temperature) GC oven (Hewlett-Packard 5890, series II) for heating. Zero time was taken  
19 when the reactors were placed in the oven. The experiments were performed at 200 and 300°C  
20 and residence times of 2, 4, 6, 8, 12 and 16 h (a total of 12 hydrochars). All runs were  
21 performed in triplicate. At the end of each experimental time, each reactor was removed from  
22 the oven and was allowed to cool in room temperature. The solid product (hydrochar) was  
23 recovered by filtration, washed with acetone and then with distilled water to remove all traces  
24 of acetone and air-dried for 24 h. From now on, the hydrochars produced will be referred to as  
25 H-temperature-residence time, e.g. H-200-2 for the sample obtained at 200°C and 2 h  
26 residence time.

27

### 28 **3 Analysis and characterization**

29 The hydrochar yield was determined as the ratio of the produced hydrochar weight (after  
30 washing and drying) to the dry weight of rice husk subjected to hydrothermal treatment:

$$31 \text{ Hydrochar yield (\%)} = (W_2/W_1) \times 100 \quad (1)$$

1 where  $W_1$  is the dry weight of the rice husk sample prior to the treatment and  $W_2$  is the  
2 hydrochar weight.

3 For measuring pH and electrical conductivity (EC) of hydrochars, suspensions of 0.01 mol/l  
4  $\text{CaCl}_2$  and distilled  $\text{H}_2\text{O}$  (1:5) were prepared. The mixtures were shaken for 1 h on a low  
5 speed shaker at room temperature. After sedimentation of hydrochar material for another  
6 hour, EC and pH were determined in the supernatant (Wiedner et al., 2013). Hydrochar  
7 nitrogen adsorption analysis to determine BET surface area and pore structure was carried out  
8 at 77 K in a Micromeritics Tristar 3000. The content in C, H, N and S was analysed by an  
9 elemental microanalyzer LECO CHNS-932 and the oxygen content was determined by  
10 difference. The parameters of yield, residence time and specific surface area were used to  
11 determine the optimum preparation conditions and the corresponding two hydrochar samples  
12 (one at each experimental temperature) to analyse further. As a result, the analyses described  
13 below were only applied to the selected hydrochars.

14 Metal content (Cu, Ni, Zn, Cd, and Pb) was determined using a Perkin Elmer 2280 atomic  
15 absorption spectrophotometer after sample extraction by digestion with 3:1 (v/v) concentrated  
16  $\text{HCl}/\text{HNO}_3$  following USEPA-3051a method (USEPA, 1997). The theoretical higher heating  
17 value ( $\text{HHV}_p$ ) was calculated using an empirical correlation developed by Channiwala and  
18 Parikh (2002)

$$19 \text{HHV}_{\text{predicted}} (\text{MJ kg}^{-1}) = 0.3491\text{C} + 1.1783\text{H} + 0.1005\text{S} - 0.1034\text{O} - 0.0015\text{N} - 0.0211\text{A} \quad (2)$$

20 Equation 2 is used to predict the HHV, where C, H, S, O, N, and A represent the weight  
21 percentages of carbon, hydrogen, sulfur, oxygen, nitrogen, and ash in hydrochars, respectively  
22 (Channiwala and Parikh, 2002). Kang et al., (2012) and He et al. (2013) used this formula and  
23 the relative error between the calculated and predicted values was less than 6%. The selected  
24 hydrochars were also subjected to derivative thermogravimetric analysis (TG-dTG) in a  
25 Labsys Setaram thermobalance under air atmosphere and  $15^\circ\text{C min}^{-1}$  heating rate. Proximate  
26 analysis was performed in the same Labsys Setaram thermobalance using  $\text{N}_2$  atmosphere and  
27  $30^\circ\text{C min}^{-1}$  heating rate. Moisture content was calculated as the weight loss from the initial  
28 temperature to  $150^\circ\text{C}$ . The volatile fraction (VM) was determined as the weight loss from  
29  $150^\circ\text{C}$  to  $600^\circ\text{C}$  under  $\text{N}_2$  atmosphere. At this temperature, air was introduced in order to  
30 determine the ash content. The fixed carbon percentage content was calculated as  $100\% -$   
31 volatile matter percentage content  $-$  ash percentage content. Fixed carbon recovery is the  
32 percent of the fixed carbon content in the biomass that is maintained in the final processed

1 product. It is an indication of the carbon sequestration potential and was determined as  
2 follows:

3 Fixed C recovery (%) = (% of fixed C in hydrochar/ % of fixed C in rice husk) x % yield (3)

4

### 5 **3 Results and Discussion**

6 The effect of temperature and residence time in hydrochar yield is presented in Figure 1. It  
7 can be seen that hydrochar yields decrease as the temperature is raised from 200 to 300°C.  
8 This decrease is closely connected with deoxygenating reactions (e.g., dehydration,  
9 decarboxylation) and volatile matter conversion, as the oxygen and hydrogen contents  
10 become lower at higher temperatures (Table 2). The hydrochar yields obtained from the  
11 hydrothermal carbonization are in the 66–58 wt.% range at 200°C and 66-36 wt.% at 300°C.  
12 At both temperatures, it can be seen that after 6 h of treatment, the yield remains somewhat  
13 constant. This indicates that any major transformations and structural rearrangements do  
14 occur in the first 6 h, after which the products became structurally stable. Gao et al. (2013)  
15 and He et al. (2013) observed the same trend during the production of hydrochars from water  
16 hyacinth and sewage sludge, respectively. The values of carbon content and surface area were  
17 used as reference points for the reproducibility of the production method. At each temperature  
18 and residence time, triplicate samples were measured in terms of carbon content and surface  
19 area and the relative standard deviation was found to be 9 and 6%, respectively.

20 The hydrothermal treatment of rice husk led to an increase in the carbon content of the solid  
21 residue from 36.1% (rice husk, Table 1) to 43 and 47% in the case of H-200-16 and H-300-  
22 16, respectively (Table 2). This shows that the rice husk was only partially carbonized during  
23 the process. The increasing trend at 300°C suggests that a more complete carbonization of the  
24 product can be achieved at longer residence times. The H/C atomic ratio decreased steadily  
25 with time, at 200°C (from 1.53 to 1.07). At 300°C, in the first 12 h the ratio is practically the  
26 same and only after 16 h a small decline was observed. This indicates that at the higher  
27 temperature the structural rearrangements and reaction pathways occur at a faster rate and the  
28 product becomes stable in a smaller amount of time. Therefore, temperature has a more  
29 predominant role than time during hydrochar production. This behaviour is consistent with  
30 the formation of a well-condensed material, especially at 300°C (Sevilla and Fuertes, 2009).

1 The pH values were acidic, approximately 4.4 and 3.4 for the 200 and 300°C hydrochars  
2 respectively. Electrical conductivity was slightly increased with temperature, from a mean of  
3 1 mS/cm at 200°C to a mean of 1.2 mS/cm at 300°C, indicating high salinity for all samples.

4 Surface areas and pore volumes were low and very similar for all hydrochar samples. The  
5 slightly increasing trend at 200°C can be attributed to the surface roughness because the pore  
6 volume remains practically the same (Unur et al., 2013). Based on the yield, residence time  
7 and surface area, two hydrochar samples were selected for further analyses. Since the yield  
8 remains nearly constant after the 6 hr mark and surface area is practically the same for all  
9 samples at both temperatures, H-200-6 and H-300-6 were selected for further tests. It is  
10 important to remember that hydrothermal treatment is an energy-consuming process, thus  
11 reducing treatment time may have a positive economic effect when scaling-up occurs.

12 Table 3 shows the results obtained from the analyses of H-200-6 and H-300-6, where an  
13 important influence of temperature can be observed. Volatile matter significantly decreased  
14 from 43.06 to 15.1 wt% in H-200-6 and H-300-6, respectively.. With respect to fixed carbon,  
15 it increased from 29.43% in H-200-6 to 46.57% in H-300-6, indicating  
16 polymerization/condensation reactions during treatment of rice husk at 300°C. These results  
17 were similar to those obtained during pyrolysis of wastes (Méndez et al., 2013). High fixed  
18 carbon recoveries (108 and 113% for the selected samples at 200 and 300°C, respectively)  
19 were obtained. Considering the principle of mass conservation, this indicates that the decrease  
20 of volatile matter at the higher temperature is converted to other products, probably CO<sub>2</sub> and  
21 other gases (Kang et al., 2012). Furthermore, it is worth mentioning that at the end of  
22 hydrothermal process, once the reactor has cooled down, there is only a slight overpressure  
23 inside the vessel, which suggests that a small amount of gaseous products are generated  
24 during hydrothermal carbonization. The heavy metal contents after acid digestion were below  
25 detection limit, except for Zn<sup>2+</sup> which increased a 65% with temperature as compared to  
26 biochars obtained by conventional pyrolysis (Méndez et al., 2012).

27 The atomic H/C and O/C ratios were calculated using the elemental composition data. Results  
28 from this analysis are presented in a Van Krevelen diagram (Fig. 2). Van Krevelen diagrams  
29 allow for delineation of reaction pathways and offer a clear insight into the chemical  
30 transformations of the carbon rich material, which are demethanation (production of  
31 methane), dehydration (production of water) and decarboxylation (production of carbonyls  
32 including carboxylic acids). Figure 2 shows that both the H/C and O/C ratios decreased when

1 the temperature was raised. At high temperature operation, the dehydration path is  
2 predominant as compared to the lower temperature operation. It is suggested that a side  
3 reaction, which is decarboxylation, occurs during the hydrothermal process because a  
4 complete dehydration reaction removes water molecules from the samples (Lu et al., 2013,  
5 Falco et al. 2011a, 2011b, Parshetti et al., 2013). Toor et al. (2011) provides a comprehensive  
6 review on the basic reaction pathways involved in the hydrothermal conversion of the main  
7 biomass components (carbohydrates, lignin, protein and lipids) to bio-products.

8 The Van Krevelen diagram suggests an improvement in the fuel properties from the H-200-6  
9 to the H-300-6 sample. This is confirmed by the predicted HHVs which indicate a 11.8%  
10 increase as the temperature is raised from 200 to 300°C (15.7 and 17.8 MJ/kg for the H-200-6  
11 and H-300-6, respectively). These values are comparable to the calorific value of lignite (16.3  
12 MJ/kg) and come in good agreement with those measured by Liu et al. (2014) for a range of  
13 hydrochars. As suggested by Danso-Boateng et al. (2013), energy densification of the  
14 hydrochars occurs as a result of decreases in solid mass caused by the dehydration and  
15 decarboxylation reactions.

16 The combustion profiles of H-200-6 and H-300-6 are shown in Figure 3. At temperatures  
17 lower than 150°C, weight loss corresponds to water release from the samples. Then, from 200  
18 to 600°C, weight loss was related with volatilization and combustion of organic matter. The  
19 dTG curve of H-200-6, showed three distinctive bands, the first related with humidity release  
20 at temperatures lower than 150°C; the second band with a maximum at 310°C was typical of  
21 cellulose combustion and finally, the third band with maximum weight loss at ~520°C could  
22 be related with combustion of more polymerized organic matter. Comparing with the H-300-6  
23 curve, the peak related with the presence of cellulose diminishes considerably whereas the  
24 peak at ~520°C slightly increases.

25 Figure 4 shows the N<sub>2</sub> isotherms for H-200-6 and H-300-6. In both cases the isotherms could  
26 be classified as type II according to the IUPAC classification. Type II isotherms are typically  
27 obtained in cases of non-porous or macroporous materials, where unrestricted monolayer-  
28 multilayer adsorption can occur. Improvements in the porosity of hydrochars and the surface  
29 area are therefore necessary to enable their use as adsorbents of contaminants, hydrogen  
30 storage or electrical energy storage (supercapacitors). Such improvements have been achieved  
31 with a combination of thermal and chemical activation methods (Sevilla et al., 2011b).

32

## 1 **4 Conclusions**

2 Rice husk was treated in subcritical water (hydrothermal carbonization) in order to obtain  
3 hydrochars. A safe and simple to set up and operate system was used, consisting of a stainless  
4 steel reactor, caps and a source of heat. Two sets of hydrochars were obtained, corresponding  
5 to experimental temperatures of 200 and 300°C and residence times in the range of 2-16 h.  
6 The carbon contents of the products increased with temperature, whereas the hydrogen and  
7 oxygen contents decreased. The surface area was low for all hydrochars, indicating that  
8 porous structure was not developed during treatment. Of the two hydrochars tested further (H-  
9 200-6 and H-300-6), the latter showed improved fuel properties as indicated by the Van  
10 Krevelen diagram and the predicted higher heating value. However, the high ash content of  
11 hydrochars from rice husk should be taken into consideration when such materials are to be  
12 used as fuels, due to potential slagging or fouling of boiler tubes and corrosion of metal  
13 surfaces. Since additional steps (such as activation) are required to increase the surface area –  
14 and therefore the adsorption capacity - of the hydrochars, their production for fuel purposes  
15 may be a more suitable pathway. The fact that hydrothermal carbonisation takes place in an  
16 aqueous reaction medium, means that wet biomass can be used, thus eliminating any energy-  
17 consuming pre-drying steps before treatment. An additional advantage is that unlike dry  
18 pyrolysis, any gaseous emissions produced during hydrothermal carbonization are largely  
19 dissolved in the char-water slurry. For this reason, hydrothermal carbonization is more  
20 flexible and has fewer technical considerations. However, there is still need for a full  
21 characterization of the acetone- and water-soluble fractions of hydrochars, in order to  
22 determine any undesirable by-products.

23

## 1 **References**

- 2 Abel, S., Peters, A., Trinks, S., Schonsky, H., Facklam, M., Wessolek, G., Impact of biochar  
3 and hydrochar addition on water retention and water repellency of sandy soil, *Geoderma* 202–  
4 203, 183–191, 2013.
- 5 Bargmann, I., Rillig, M. C., Buss, W., Kruse, A., Kuecke, M., Hydrochar and biochar effects  
6 on Germination of Spring Barley, *Journal of Agronomy and Crop Science* 199, 360-373,  
7 2013.
- 8 Busch, D., Stark, A., Kammann, C.I., Glaser, B., Genotoxic and phytotoxic risk assessment of  
9 fresh and treated hydrochar from hydrothermal carbonization compared to biochar from  
10 pyrolysis, *Ecotoxicology and Environmental Safety* 97, 59–66, 2013.
- 11 Channiwala, S. A., Parikh, P.P., A unified correlation for estimating HHV of solid, liquid and  
12 gaseous fuels, *Fuel* 81, 1051 – 1063, 2002.
- 13 Danso-Boateng, E., Holdich, R.G., Shama, G., Wheatley, A.D., Sohail, M., Martin, S.J.,  
14 Kinetics of faecal biomass hydrothermal carbonisation for hydrochar production, *Applied*  
15 *Energy* 111, 351–357, 2013.
- 16 Daskalaki, V.M., Timotheatou E.S., Katsaounis, A., Kalderis, D., Degradation of Reactive  
17 Red 120 using hydrogen peroxide in subcritical water, *Desalination* 274, 200–205, 2011.
- 18 Ding, L., Zou, B., Li, Y., Liu, H., Wang, Z., Zhao, C., Su, Y., Guo, Y., The production of  
19 hydrochar-based hierarchical porous carbons for use as electrochemical supercapacitor  
20 electrode materials, *Colloids and Surfaces A: Physicochemical and Engineering Aspects* 423,  
21 104-111, 2013a.
- 22 Ding, L., Zou, B., Liu, H., Li, Y., Wang, Z., Su, Y., Guo, Y., Wang, X., A new route for  
23 conversion of corncob to porous carbon by hydrolysis and activation, *Chemical Engineering*  
24 *Journal* 225, 300–305, 2013b.
- 25 Falco, C., Baccile, N., Titirici, M.-M., Morphological and structural differences between  
26 glucose, cellulose and lignocellulosic biomass derived hydrothermal carbons, *Green*  
27 *Chemistry* 13, 3273–3281. 2011a.
- 28 Falco, C., Caballero, F.P., Babonneau, F., Gervais, C., Laurent, G., Titirici, M.M., Baccile,  
29 N., Hydrothermal carbon from biomass: structural differences between hydrothermal and  
30 pyrolyzed carbons via <sup>13</sup>C solid state NMR, *Langmuir* 27, 14460–14471, 2011b.

- 1 Gajić, A., and Koch H.-J., Sugar beet (*Beta vulgaris* L.) growth reduction caused by  
2 hydrochar is related to nitrogen supply, *Journal of Environmental Quality* 41, 1067–1075,  
3 2012.
- 4 Gao, Y., Wang, X., Wang, J., Li, X., Cheng, J., Yang, H., Chen, H., Effect of residence  
5 time on chemical and structural properties of hydrochar obtained by hydrothermal  
6 carbonization of water hyacinth, *Energy* 58, 376-383, 2013.
- 7 He, C., Giannis, A., Wang, J.-Y., Conversion of sewage sludge to clean solid fuel using  
8 hydrothermal carbonization: Hydrochar fuel characteristics and combustion behaviour,  
9 *Applied Energy* 111, 257–266, 2013.
- 10 Jamari, S.S., and Howse, J.R., The effect of the hydrothermal carbonization process on palm  
11 oil empty fruit bunch, *Biomass and Bioenergy* 47, 82-90, 2012.
- 12 Kalderis, D., Hawthorne, S.B., Clifford, A.A., Gidarakos, E., Interaction of soil, water and  
13 TNT during degradation of TNT on contaminated soil using subcritical water, *J. Hazard.*  
14 *Materials* 159, 329-334, 2008.
- 15 Kang, S., Li, X., Fan, J., and Chang, Ji., Characterization of hydrochars produced by  
16 hydrothermal Carbonization of lignin, cellulose, D-xylose, and wood meal, *Industrial and*  
17 *Engineering Chemistry Research* 51, 9012-9023, 2012.
- 18 Liu, Z., Quek, A., Kent Hoekman, S., and Balasubramanian, R., Production of solid biochar  
19 fuel from waste biomass by hydrothermal carbonization, *Fuel* 103, 943-949, 2013.
- 20 Liu, Z., Quek, A., and Balasubramanian, R., Preparation and characterization of fuel pellets  
21 from woody biomass, agro-residues and their corresponding hydrochars, *Applied Energy* 113,  
22 1315–1322, 2014.
- 23 Lu, X., Pellechia, P.J., Flora, J.R.V., Berge, N.D., Influence of reaction time and temperature  
24 on product formation and characteristics associated with the hydrothermal carbonization of  
25 cellulose, *Bioresource Technology* 138, 180–190, 2013.
- 26 Méndez, A., Gómez, A., Paz-Ferreiro, J., Gascó, G., Effects of sewage sludge biochar on  
27 plant metal availability after application to a Mediterranean soil, *Chemosphere* 89(11), 1354-  
28 1359, 2012.

1 Méndez, A., Terradillos, M., Gascó, G., Physicochemical and agronomic properties of biochar  
2 from sewage sludge pyrolysed at different temperatures, *Journal of Analytical and Applied*  
3 *Pyrolysis* 102, 124-130, 2013.

4 Parshetti, G.K., Kent Hoekman, S., Balasubramanian, R., Chemical, structural and  
5 combustion characteristics of carbonaceous products obtained by hydrothermal carbonization  
6 of palm empty fruit bunches, *Bioresource Technology* 135, 683-689, 2013.

7 Sevilla, M., and Fuertes, A.B., The production of carbon materials by hydrothermal  
8 carbonization of cellulose, *Carbon* 47, 2281-2289, 2009.

9 Sevilla, M., Macia-Agullo, J.A., Fuertes, A.B., Hydrothermal carbonization of biomass as a  
10 route for the sequestration of CO<sub>2</sub>: Chemical and structural properties of the carbonized  
11 products, *Biomass and Bioenergy* 35, 3152-3159, 2011a.

12 Sevilla, M., Fuertes, A.B., Mokaya, R., High density hydrogen storage in superactivated  
13 carbons from hydrothermally carbonized renewable organic materials. *Energy Environ. Sci.* 4,  
14 1400–1410, 2011b.

15 Toufiq Reza, M., Lynam J.G., Helal Uddin, M., Coronella, C.J., Hydrothermal carbonization:  
16 Fate of inorganics, *Biomass and Bioenergy* 49, 89-94, 2013.

17 Toor, S.S., Rosendahl, L., Rudolf, A., Hydrothermal liquefaction of biomass: A review of  
18 subcritical water technologies, *Energy* 36, 2328-2342, 2011.

19 Unur, E., Brutti, S., Panero S., Scrosati, B., Nanoporous carbons from hydrothermally treated  
20 biomass as anode materials for lithium ion batteries, *Microporous and Mesoporous Materials*  
21 174, 25-33, 2013.

22 USEPA. 1997. Method 3051a: Microwave assisted acid dissolution of sediments, sludges,  
23 soils and oils. 2<sup>o</sup> ed. U.S. Gov. Print. Office. Washington. USA.

24 Wagner, A., and Kaupenjohann, M., Suitability of biochars (pyro- and hydrochars) for metal  
25 immobilization on former sewage-field soils, *European Journal of Soil Science* 65, 139-148,  
26 2014.

27 Wiedner, K., Naisse, C., Rumpel C., Pozzi A., Wieczorek, P., Glaser, B., Chemical  
28 modification of biomass residues during hydrothermal carbonization – What makes the  
29 difference, temperature or feedstock?, *Organic Geochemistry* 54, 91-100, 2013.

30

1

2 **Table 1.** Properties of the rice husk (used in this study) and rice husk ash

<b>Rice husk</b>	
Moisture (%)	4.2
Ash content (%)	16.1
Volatile matter (%)	62
Carbon (%)	36.1
Fixed carbon (%)	17.7
Higher heating value (MJ/kg)	15.1

<b>Rice husk ash</b>	wt. %
SiO <sub>2</sub>	84.7
K <sub>2</sub> O	2.51
CaO	0.74
Al <sub>2</sub> O <sub>3</sub>	0.36
Na <sub>2</sub> O	0.20
MgO	0.76
P <sub>2</sub> O <sub>5</sub>	0.62
SO <sub>3</sub>	0.38
Fe <sub>2</sub> O <sub>3</sub>	0.28
Cl	0.18

3

4

5

6

7

1

2 **Table 2.** Characterization of the hydrochar samples obtained at 200 and 300°C

	pH	EC (mS)	C <sup>2</sup> (%)	H (%)	N (%)	S (%)	H/C atomic ratio	Surface area <sup>2</sup> (m <sup>2</sup> /g)	Pore volume (cm <sup>3</sup> /g)
H-200-2	4.42	0.98	37.82	4.82	0.34	0.05	1.53	14.6	0.034
H-200-4	4.34	1.01	39.83	4.51	0.40	0.04	1.36	19.4	0.056
H-200-6 <sup>1</sup>	4.19	1.02	40.81	4.31	0.44	0.04	1.27	20.7	0.064
H-200-8	4.22	1.01	42.6	4.17	0.50	0.08	1.17	21.5	0.076
H-200-12	4.33	0.99	44.08	4.06	0.53	0.01	1.11	22.6	0.092
H-200-16	4.35	0.98	43.13	3.83	0.53	0.02	1.07	29.7	0.128
H-300-2	3.41	1.18	41.87	2.97	0.62	0.01	0.85	14.5	0.065
H-300-4	3.43	1.23	42.43	3.55	0.64	0.06	0.84	24.9	0.082
H-300-6 <sup>1</sup>	3.41	1.35	45.56	3.2	0.69	0.04	0.84	20.3	0.074
H-300-8	3.41	1.17	46.01	3.26	0.75	0.03	0.85	19.1	0.069
H-300-12	3.46	1.34	46.19	3.26	0.75	0.03	0.85	23.3	0.073
H-300-16	3.43	1.36	47.32	3.13	0.74	0.04	0.79	18.7	0.049

3 1. these samples were selected for further analyses

4 2. average values of triplicate measurements

5

6

7

8

9

10

11

1 **Table 3.** Properties of hydrochar samples H-200-6 and H-300-6

	<b>H-200-6</b>	<b>H-300-6</b>
Volatile organic content VM (%)	43.06	15.10
Fixed carbon content FC (%)	29.43	46.57
Fixed carbon recovery (%)	108	113
Ash content (%)	24.54	40.14
Micropore area (m <sup>2</sup> /g)	0.8714	1.0036
HHV predicted (MJ/kg)	15.7	17.8
O (%) <sup>1</sup>	29.86	10.37
Cu (mg kg <sup>-1</sup> )	nd <sup>2</sup>	nd
Ni (mg kg <sup>-1</sup> )	nd	nd
Cd (mg kg <sup>-1</sup> )	nd	nd
Zn (mg kg <sup>-1</sup> )	0.80	1.32
Pb (mg kg <sup>-1</sup> )	nd	nd

2 1. calculated by difference

3 2. non-detected

4

5

6

7

8

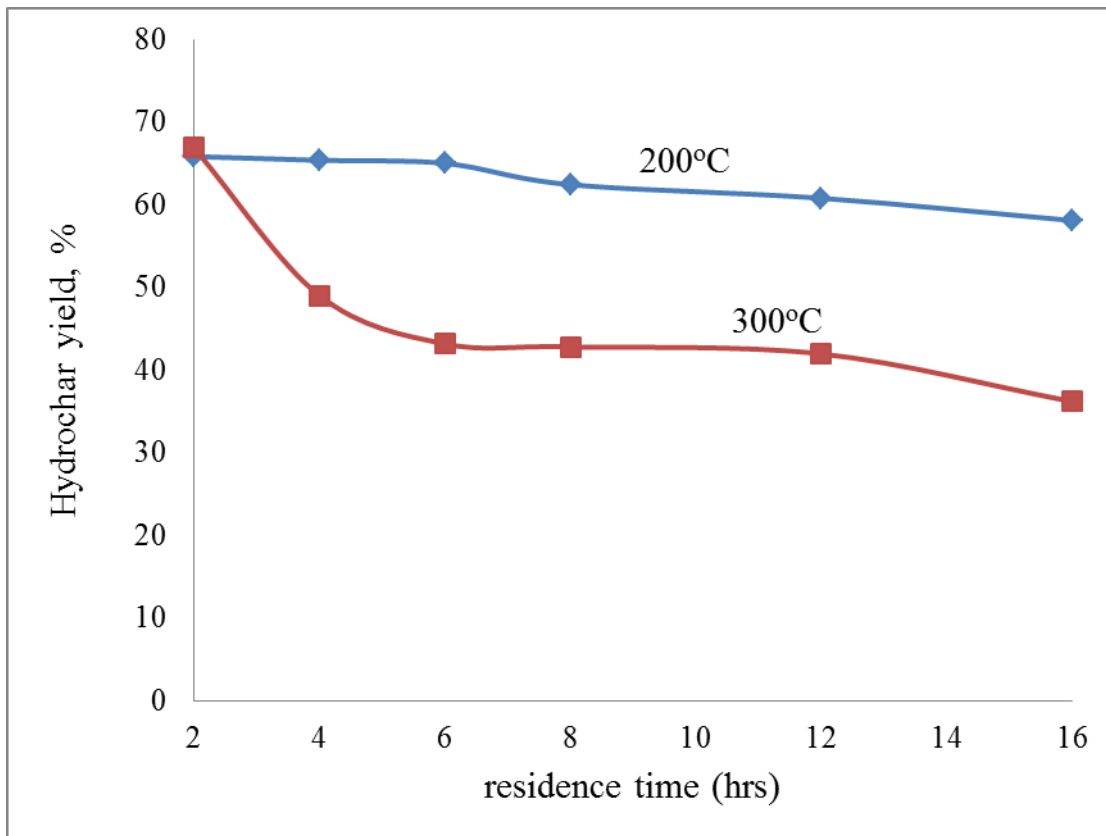
9

10

11

12

13

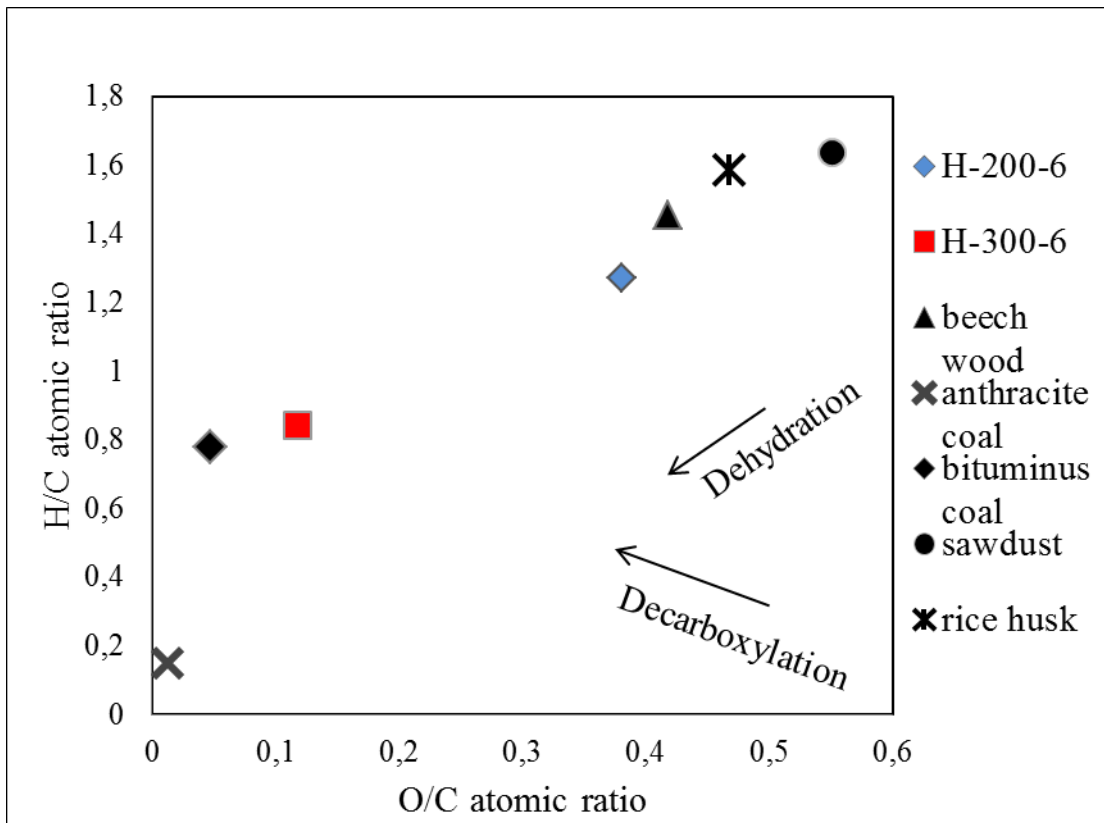


1

2 **Figure 1.** Hydrochar yields

3

4



1

2 **Figure 2.** Van Krevelen diagram showing the position of H-200-6 and H-300-6 hydrochars  
 3 among known fuels and biomass materials

4

5

6

7

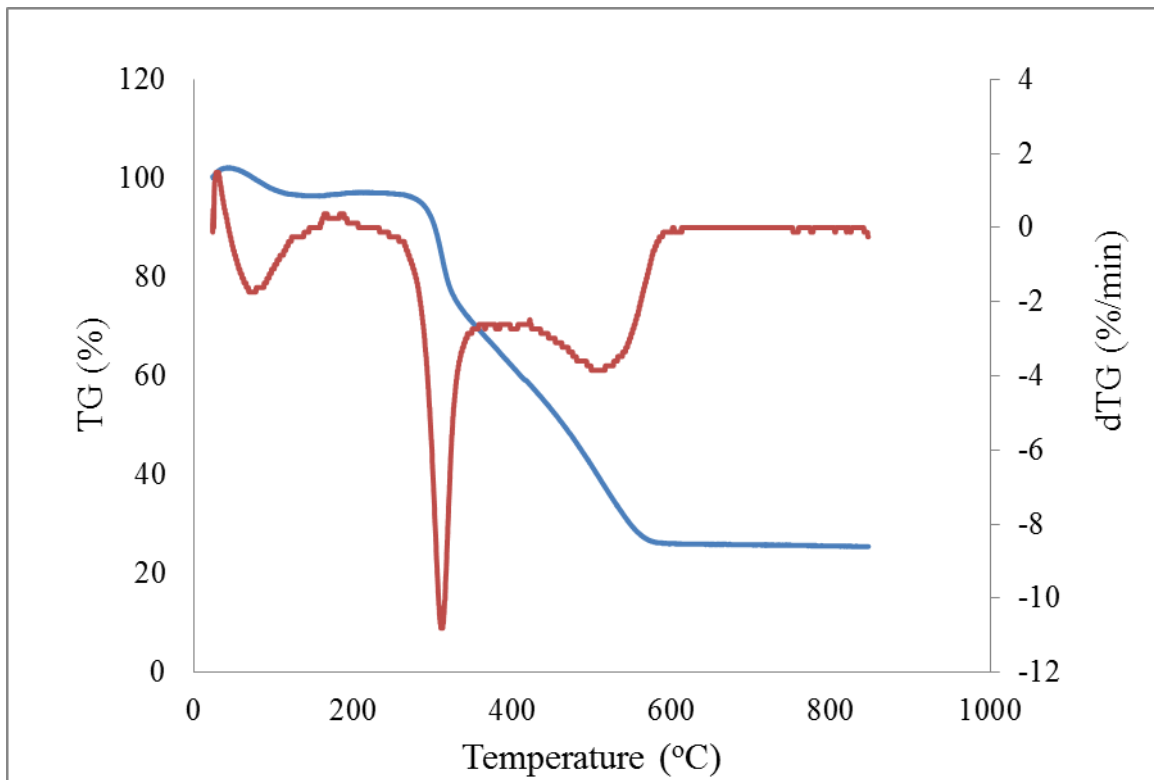
8

9

10

11

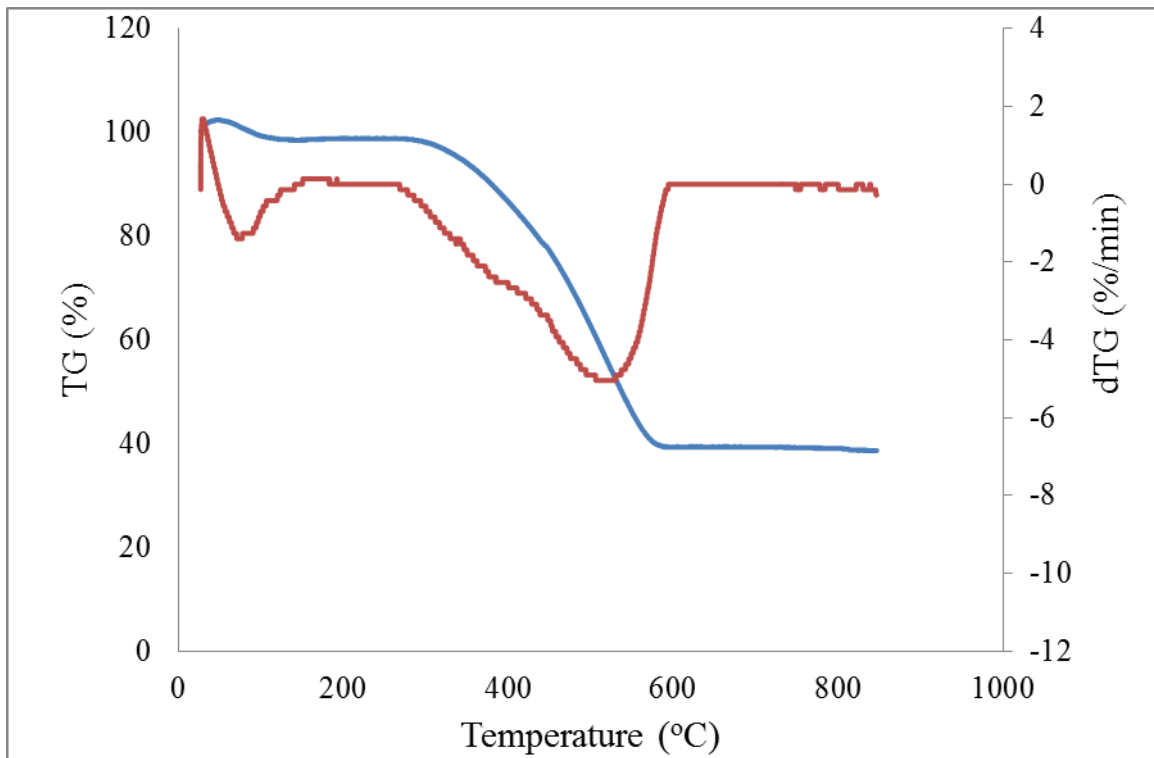
12



1

2

(a)



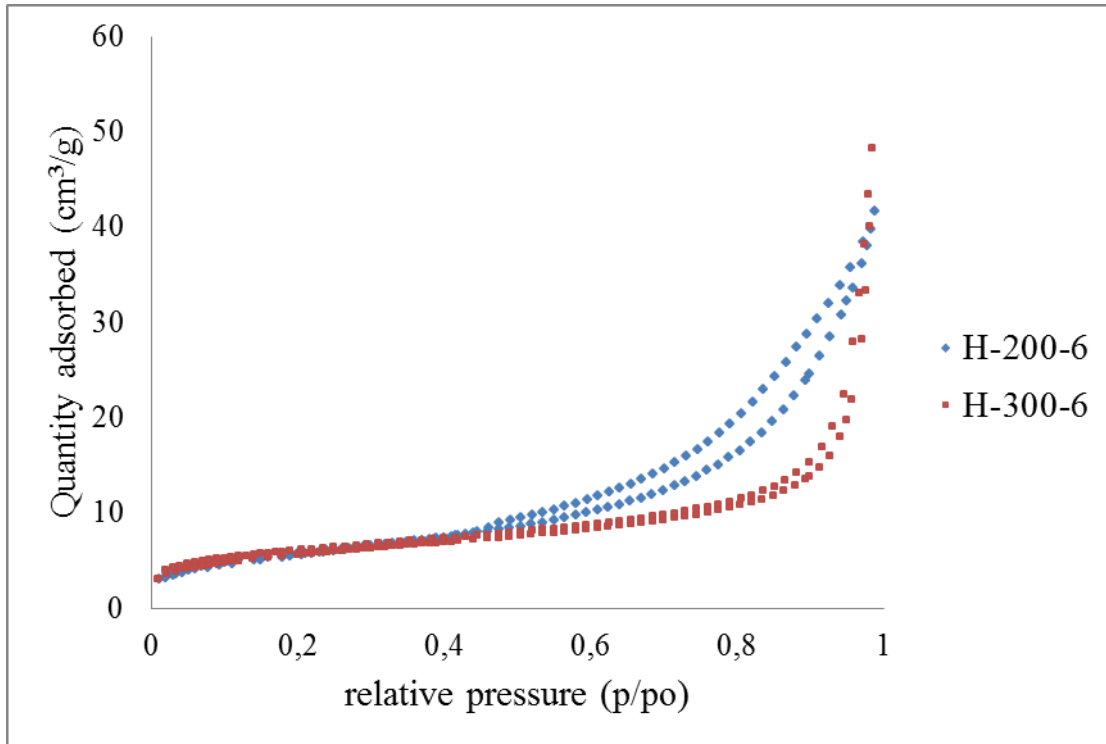
3

4

(b)

5 **Figure 3.** TG-dTG curves for the combustion profiles of (a) H-200-6 and (B) H-300-6

1



2

3 **Figure 4.** Nitrogen adsorption and desorption isotherms for H-200-6 and H-300-6

4

5

6

7

8

9

10

11

12

13

14

15

16

